Lesser, D. R., Kurpiewski, M. R., & Jen-Jacobson, L. (1990) *Science 250*, 776-786.
Lu, A.-L., Jack, W., & Modrich, P. (1981) *J. Biol. Chem. 256*, 13200-13206.
Luke, P. A., & Halford, S. E. (1985) *Gene 37*, 241-246.
McClarin, J. A., Frederick, C. A., Wang, B.-C., Greene, P., Boyer, H. W., Grable, J., & Rosenberg, J. M. (1986) *Science 234*, 1526-1541.
McLaughlin, L. W., Benseler, F., Graeser, E., Piel, N., & Scholtissek, S. (1987) *Biochemistry 26*, 7238-7245.
Modrich, P., & Zabel, D. (1976) *J. Biol. Chem. 251*, 5866-5874.
Modrich, P., & Roberts, R. J. (1982) in *Nucleases* (Linn, S. M., & Roberts, R. J., Eds.) pp 109-154, Cold Spring Harbor Laboratory, Cold Spring Harbor, NY.
Mossing, M. C., & Record, M. T. (1985) *J. Mol. Biol. 186*, 295-305.
Nerdal, W., Hare, D. R., & Reid, B. R. (1989) *Biochemistry 28*, 10008-10021.
Newman, A. K., Rubin, R. A., Kim, S.-H., & Modrich, P. (1981) *J. Biol. Chem. 256*, 2131-2139.
Patel, D., Pardi, A., & Itakura, K. (1982) *Science 216*, 581-590.
Rosenberg, J. M. (1991) *Curr. Opin. Struct. Biol. 1*, 104-113.
Rosenberg, J. M., McClarin, J. A., Frederick, C. A., Grable, J., & Boyer, H. W. (1987) in *Gene Amplification and Analysis*, (Chirikjian, J., Ed.) Vol. 5, pp 119-145, Elsevier/North-Holland, New York.
Rubin, R. A., & Modrich, P. (1978) *Nucleic Acids Res. 5*, 2991-2997.
Terry, B., Jack, W., & Modrich, P. (1987) in *Gene Amplification and Analysis* (Chirikjian, J., Ed.) Vol. 5, pp 103-118, Elsevier/North-Holland, New York.
Theilking, U., Alves, J., Fliess, A., Maass, G., & Pingoud, A. (1990) *Biochemistry 29*, 4682-4691.
Thomas, M., & Davis, R. (1975) *J. Mol. Biol. 91*, 315-328.
Thomas, G. A., Kubasek, W. L., Peticolas, W. L., Greene, P., Grable, J., & Rosenberg, J. M. (1989) *Biochemistry 28*, 2001-2009.
Voight, J. M., & Topal, M. O. (1990) *Biochemistry 29*, 1632-1637.
Wells, R. D., Klein, R. D., & Singleton, C. K. (1981) *Enzymes (3rd Ed.) 14*, 177-182.
Yolov, A., Gromova, E., Kubareva, E., Potapov, V., & Shabarova, Z. (1985) *Nucleic Acids Res. 13*, 8969-8981.

Proton NMR Studies of [*N*-MeCys^3,*N*-MeCys^7]TANDEM Binding to DNA Oligonucleotides: Sequence-Specific Binding at the TpA Site†

Kenneth J. Addess,‡ Dara E. Gilbert,‡ Richard K. Olsen,§ and Juli Feigon*,‡
Department of Chemistry and Biochemistry and Molecular Biology Institute, University of California, Los Angeles, California 90024, and Department of Chemistry and Biochemistry, Utah State University, Logan, Utah 84322
Received July 24, 1991; Revised Manuscript Received October 3, 1991

ABSTRACT: [*N*-MeCys^3,*N*-MeCys^7]TANDEM, an undermethylated analogue of Triostin A, contains two *N*-methyl groups on the cysteine residues only. Footprinting results showed that [*N*-MeCys^3,*N*-MeCys^7]TANDEM binds strongly to DNA rich in A·T residues [Low, C. M. L., Fox, K. R., Olsen, R. K., & Waring, M. J. (1986) *Nucleic Acids Res. 14*, 2015-2033]. However, it was not known whether specific binding of [*N*-MeCys^3,*N*-MeCys^7]TANDEM requires a TpA step or an ApT step. In 1:1 saturated complexes with the octamers $[d(GGATATCC)]_2$ and $[d(GGTTAACC)]_2$, [*N*-MeCys^3,*N*-MeCys^7]TANDEM binds to each octamer as a bis-intercalator bracketing the TpA step. The octadepsipeptide ring binds in the minor groove of the DNA. Analysis of sugar coupling constants from the phase-sensitive COSY data indicates that the sugar of the thymine in the TpA binding site adopts predominantly an N-type sugar conformation, while the remaining sugars on the DNA adopt an S-type conformation, as has been observed in other Triostin A and echinomycin complexes. The drug does not bind to the octamer $[d(GGAATTCC)]_2$ as a bis-intercalator. Only weak nonintercalative binding is observed to this DNA octamer. These results show unambiguously that [*N*-MeCys^3,*N*-MeCys^7]TANDEM binds sequence specifically at TpA sites in DNA. The factors underlying the sequence specificity of [*N*-MeCys^3,*N*-MeCys^7]TANDEM binding to DNA are discussed.

[*N*-MeCys^3,*N*-MeCys^7]TANDEM[1] is a cyclic octadepsipeptide antibiotic that contains a disulfide cross bridge and two quinoxaline rings attached to two D-Ser residues (Chart I). [*N*-MeCys^3,*N*-MeCys^7]TANDEM (hereafter referred to as CysMeTANDEM) is a methylated analogue of the undermethylated TANDEM (des-*N*-tetramethyl-Triostin A). CysMeTANDEM is also an undermethylated analogue of the naturally occurring antibiotic Triostin A, which contains *N*-methyl substituents on the Cys and Val residues. Triostin A and its two synthetic analogues belong to a class of antibiotics called triostins. Echinomycin, which also contains

† This work was supported by grants from the NIH (R01 GM 37254-01) and by a NSF Presidential Young Investigator Award (DMB 89-58280) with matching funds from AmGen Inc., Du Pont/Merck Pharmaceuticals, Monsanto Co., and Sterling Drug Inc. D.E.G. was supported in part by an NIH Predoctoral Cell and Molecular Biology training grant (GM 07185).
‡ University of California, Los Angeles.
§ Utah State University.

[1] Abbreviations: 2D NMR, two-dimensional nuclear magnetic resonance spectroscopy; [*N*-MeCys^3,*N*-MeCys^7]TANDEM; CysMeTANDEM; COSY, correlation spectroscopy; HOHAHA, homonuclear Hartmann-Hahn spectroscopy; *N*-MeCys, *N*-methylcysteine; NOESY, nuclear Overhauser effect spectroscopy; P.E.COSY, primitive exclusive COSY; P.COSY, purged COSY.

0006-2960/92/0431-339$03.00/0

Chart I: Chemical Structure of CysMeTANDEM

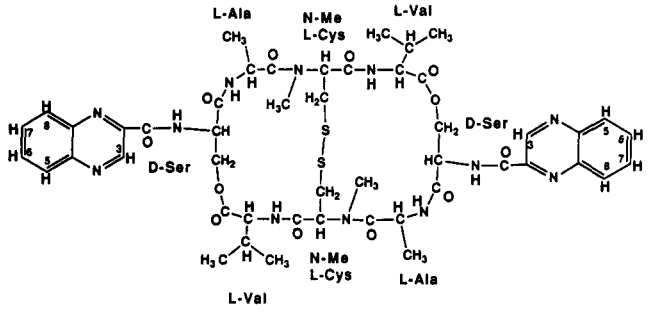

N-methyl substituents on the Val and Cys residues, has a thioacetal cross bridge and belongs to a family of quinoxaline antibiotics called quinomycins (Katagiri et al., 1975; Waring, 1979). These drugs show potent antitumor and antibiotic activity (Katagiri et al., 1975). Early studies on the binding of echinomycin, Triostin A, and TANDEM to natural DNAs with varying percent G·C content and to synthetic polymers indicated that while echinomycin and Triostin A showed a marked preference for G·C-rich DNA (Lee & Waring, 1978a), TANDEM preferentially bound alternating A·T sequences (Lee & Waring, 1978b). DNA unwinding assays with these drugs also indicated that they bound to DNA by bis-intercalation (Fox et al., 1982; Lee & Waring, 1978a,b; Wakelin & Waring, 1974).

Footprinting studies with DNase I (Low et al., 1984a,b) and MPE–Fe(II) (van Dyke & Dervan, 1984) showed that the preferred binding sites for echinomycin and Triostin A are centered around a CpG step. Crystal structures and NMR studies of complexes between DNA and echinomycin and Triostin A have provided direct evidence for how these drugs bind to DNA (Gao & Patel, 1988; Gilbert et al., 1989; Gilbert & Feigon, 1991; Ughetto et al., 1985; Wang et al., 1984, 1986). These studies indicated that echinomycin and Triostin A bis-intercalate on either side of a CpG step with the peptide ring positioned in the minor groove of the DNA.

Less is known about how TANDEM and CysMeTANDEM interact with DNA and why they preferentially bind A·T-rich DNA. DNase I footprinting studies of TANDEM bound to a 160 base pair restriction fragment showed two binding sites centered around A-T-A or T-A-T (Low et al., 1984b). The difference in binding site preferences between TANDEM and echinomycin or Triostin A was attributed to the *N*-methyl substituents on the Val and Cys residues of the octadepsipeptide ring, since these are the only common chemical difference between the former and latter. The effect of the Cys *N*-methyl groups on the sequence specificity of TANDEM was directly addressed by Low et al. (1986) using the analogue CysMeTANDEM. DNase I footprinting of CysMeTANDEM (Low et al., 1986) gave a virtually identical footprint of a DNA fragment to that observed with TANDEM (Low et al., 1984b). Both molecules bind quite strongly to A·T-rich regions of DNA. Waring and co-workers also found that CysMeTANDEM inhibits the activity of the enzyme *Rsa*I, which restricts GTAC, but does not affect the activity of *Sau*3AI, which restricts the GATC site (Low et al., 1986). These results suggested, but did not prove unambiguously, that CysMeTANDEM prefers a TpA site to an ApT site and that the cysteine *N*-methyl plays little or no role in the drug's preference for A·T rich DNA.

To date, relatively little has been published on the structure of TANDEM–DNA or CysMeTANDEM–DNA complexes. The crystal structure of TANDEM alone has been reported (Viswamitra et al., 1981). On the basis of the crystal structure,

Chart II: Sequence and Numbering System of the Two DNA Oligonucleotides with the Orientation of the Bound CysMeTANDEM Shown Schematically

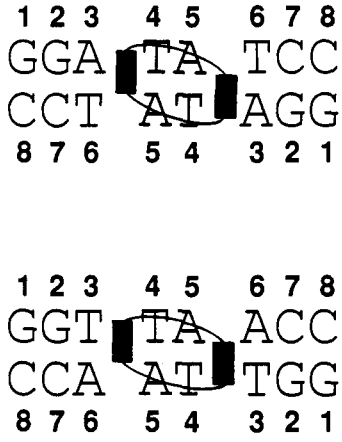

the authors proposed that TANDEM should bis-intercalate specifically at ApT sequences. Proton and phosphorous NMR studies of the interaction between CysMeTANDEM and the decamer $[d(CCCGATCGGG)]_2$ have been reported (Powers et al., 1989). The authors found no evidence for intercalative binding of CysMeTANDEM to this sequence and proposed a model for the drug–DNA complex in which the two quinoxaline rings bind in the minor groove of the DNA.

In order to better understand the interaction of TANDEM and CysMeTANDEM with A·T-rich DNA and to obtain more information about its binding site requirements, we have investigated the binding of CysMeTANDEM to the DNA octamers $[d(GGATATCC)]_2$, $[d(GGTTAACC)]_2$, and $[d(GGAATTCC)]_2$ using ^1H NMR spectroscopy. In this paper, we present direct evidence that CysMeTANDEM binds specifically to a TpA step as indicated in Chart II. For CysMeTANDEM complexed to $[d(GGATATCC)]_2$ and $[d(GGTTAACC)]_2$, bis-intercalation around the TpA binding site is observed. In contrast, CysMeTANDEM binds weakly to [d(GGAATTCC)], and the binding is not intercalative. This indicates unambiguously that a TpA step and not an ApT step is required for specific binding. Analysis of the NMR spectra of the complexes of CysMeTANDEM with $[d(GGATATCC)]_2$ and $[d(GGTTAACC)]_2$ shows similar contacts between the octadepsipeptide ring and the DNA in both complexes. In addition, binding of CysMeTANDEM to both the octamers containing a TpA step (ATAT and TTAA) causes the T sugar of the TpA step of each complex to adopt mainly an N-type geometry, as has also been observed in drug–DNA complexes with CpG-specific drugs such as Triostin A (Wang et al., 1984, 1986) and echinomycin (Gao & Patel, 1988; Gilbert et al., 1989; Gilbert & Feigon, 1991; Ughetto et al., 1985).

Materials and Methods

Sample Preparation. The octamers $d(G_1G_2A_3T_4A_5T_6C_7C_8)$, $d(G_1G_2T_3T_4A_5A_6C_7C_8)$, and $d(G_1G_2A_3A_4T_5T_6C_7C_8)$ were synthesized on an ABI 381A synthesizer using β-cyanoethyl phosphoramidite chemistry on a 10-μmol scale. All oligonucleotides were purified by gel filtration by the method of Kintanar et al. (1987). The samples contained ~2 mM DNA duplex and 150 mM NaCl at pH 6.5. The DNA samples were lyophilized twice in 99.96% D_2O, dried a third time in the NMR tube with a stream of nitrogen, and dissolved in 400 μL of 99.996% D_2O. Spectra in H_2O were taken on the sample after redrying the NMR tube with $N_{2(g)}$ and redissolving in 90% H_2O/10% D_2O.

CysMeTANDEM was synthesized using procedures developed for TANDEM and Triostin A (Chakravarty & Olsen, 1978; Olsen et al., 1986). Drug–DNA complexes were made by adding appropriate amounts of CysMeTANDEM dissolved in methanol to the DNA sample in the NMR tube. The concentration of the CysMeTANDEM solutions in methanol was determined from UV absorbance at 325 nm, using the ϵ_{325} for TANDEM, which is equal to 12 130 cm^{-1} M^{-1} (Low et al., 1984a). The methanol and water were then evaporated over a period of 12–18 h under a stream of $N_{2(g)}$, and the sample was redissolved in 400 μL of D_2O. For the fully saturated complexes, CysMeTANDEM solutions were added to the DNA until no more drug would dissolve, i.e., excess drug precipitated during the drying period and would not redissolve. Complex formation was monitored by NMR. For experiments in D_2O, the dried samples were redried and redissolved in 99.996% D_2O. For spectra in H_2O, the dried samples were redissolved in 90% H_2O/10% D_2O.

NMR Spectroscopy. All NMR experiments were done on a General Electric GN500 (500.119 MHz, ^1H) spectrometer. Phase-sensitive nuclear Overhauser effect (NOESY) (Kumar et al., 1980) spectra in D_2O were obtained using the method of States et al. (1982) with preirradiation of the HDO peak during the recycle delay. Phase-sensitive NOESY spectra in H_2O were obtained by replacing the last 90° pulse with a $1\bar{1}$ spin echo pulse sequence and phase cycling appropriately in to order to suppress the large water resonance (Sklenář & Bax, 1987). The carrier was centered at the water resonance, and the delay τ was adjusted so that the excitation maximum was at ~12 ppm (τ = 60 μs, Δ = 50 μs). HOHAHA spectra were acquired using the MLEV 17 mixing sequence and two 1.5-ms trim pulses for the spin lock (Bax & Davis, 1985). Magnitude COSY spectra were acquired with the standard pulse sequence and phase cycling (Aue et al., 1976). P.COSY spectra were acquired with a mixing pulse of 90° (Marion & Bax., 1988). P.E.COSY spectra were acquired with a mixing pulse of 35° (Mueller, 1987). All 2D NMR spectra were processed on a VAX 8820 or a Personal Iris 4D25 using the Fortran program FTNMR (Hare Research). NOESY spectra were baseline flattened with a first-order polynomial in t_2 and with a second-order polynomial in t_1. T_1 ridge noise was minimized by multiplying the first row by one half (Otting et al., 1986). Detailed description of the acquisition and processing parameters for other experiments are given in the figure captions.

Measurement of Coupling Constants. The values of $J_{1'2'}$ and $J_{1'2''}$ coupling constants were initially measured directly from the P.E.COSY spectrum (Bax & Lerner, 1987). The measured coupling constants were then used as starting values for computer simulation of the H1′–H2′,H2″ region of the P.COSY spectrum using the programs SPHINX and LINSHA (Widmer & Wüthrich, 1987). For these simulations, $J_{1'2'}$, $J_{1'2''}$, $J_{2'3'}$, and $J_{2''3'}$ were all independently varied, and $J_{2'2''}$ was held constant at −14 Hz (Widmer & Wüthrich, 1987). The $J_{1'2'}$ and $J_{1'2''}$ coupling constants were used to estimate each sugar conformation assuming a two-site model as described by Rinkel and Altona (1987) in which sugars in solution exist in fast equilibrium between the S-type conformation (near C2′ endo) and the N-type conformation (near C3′ endo). According to this model, the fraction of S conformation can be calculated from the sum of the H1′ coupling constants ($\sum 1' = J_{1'2} + J_{1'2''}$) using the equation $p\mathrm{S} = (\sum 1' - 9.8)/5.9$.

RESULTS

CysMeTANDEM–DNA Complex Formation. One-dimensional ^1H NMR spectra of $[d(GGATATCC)]_2$ and $[d(GGTTAACC)]_2$ containing no drug and one drug per DNA duplex in D_2O are shown in Figure 1a,b and Figure 1c,d, respectively. For each complex, addition of one equivalent of drug to the DNA results in the appearance of new resonances, which belong to the bound drug, plus a shift in the DNA resonances as a consequence of complex formation. The change in the spectra from free duplex to the complex is illustrated by the shift in the thymine methyl resonances and the appearance of the Ala methyl, Val methyl, Cys *N*-Me, and the slowly exchanging Val amide resonances labeled in Figure 1. For the free DNA, the two strands of each of the two duplexes are symmetrical in solution, giving rise to only one resonance line for each of the protons on the symmetry-related bases. No doubling of the DNA and drug resonances are observed for the fully saturated complexes, indicating that both the DNA and the drug retain their 2-fold symmetry on complex formation. At less than saturating drug–DNA ratios, for both DNA oligonucleotides, two separate sets of resonance lines appear, corresponding to the free DNA and the 1:1 drug–DNA complex (spectra not shown). This indicates that for each complex the drug is in slow exchange with the DNA on the NMR time scale.

Imino proton spectra of the free DNA and the two 1:1 drug–DNA complexes in H_2O are shown in Figure 2a–d.

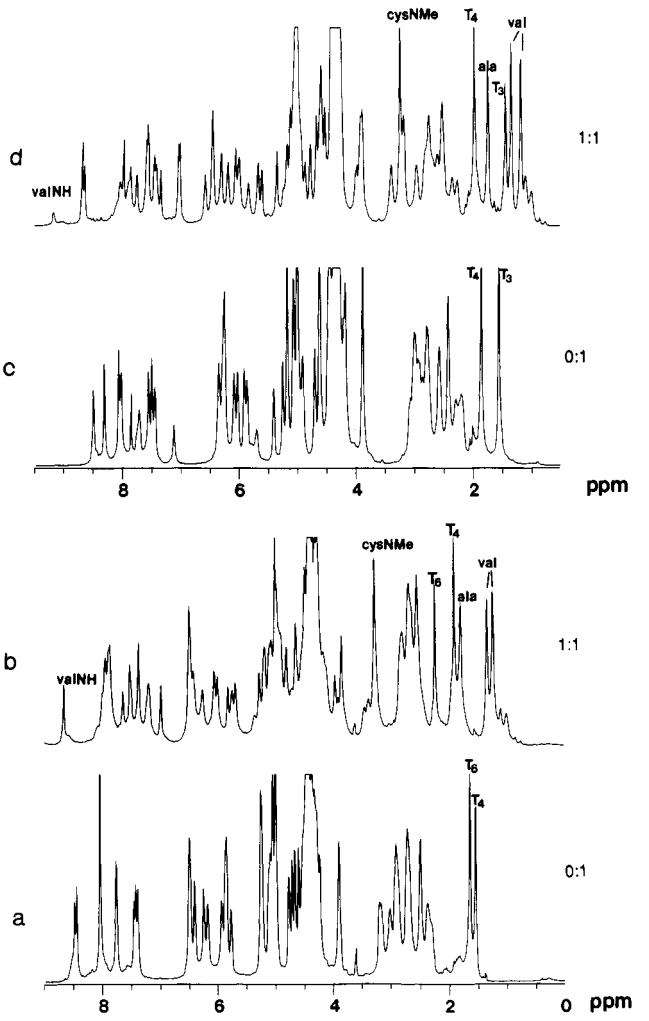

FIGURE 1: One-dimensional ^1H NMR spectra of (a) $[d(GGATATCC)]_2$, (b) 1:1 complex of CysMeTANDEM + $[d(GGATATCC)]_2$, (c) $[d(GGTTAACC)]_2$, and (d) 1:1 complex of CysMeTANDEM + $[d(GGTTAACC)]_2$ in D_2O at 25 °C. Samples are 2 mM DNA duplex and 150 mM NaCl, pH 6.5. Assignments of the thymine methyls, the Ala methyl, the Val methyls, and the Val NH are indicated. The spectra were acquired with a sweep width of 5000 Hz in 2K complex points and were line broadened by 3 Hz prior to Fourier transformation.

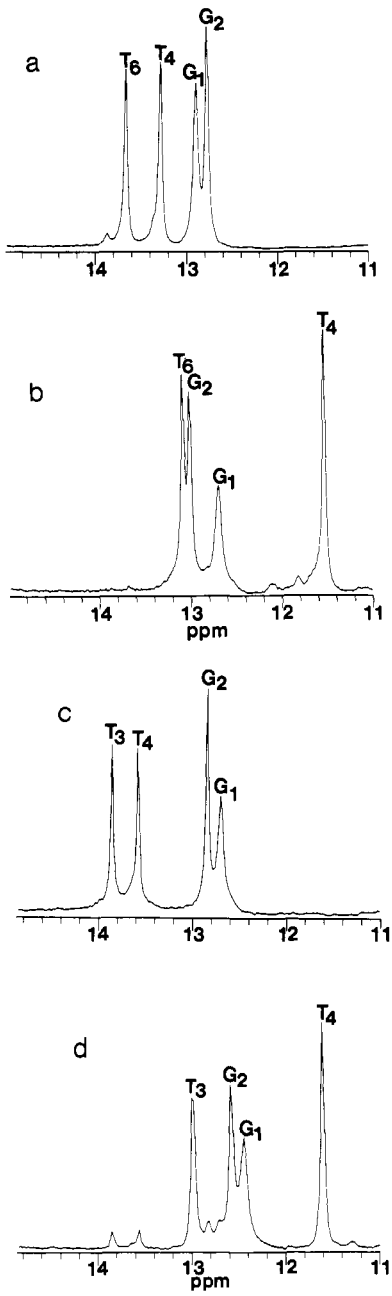

FIGURE 2: Imino proton spectra of (a) $[d(GGATATCC)]_2$, (b) 1:1 complex of CysMeTANDEM + $[d(GGATATCC)]_2$, (c) $[d(GGTTAACC)]_2$, and (d) 1:1 complex of CysMeTANDEM + $[d(GGTTAACC)]_2$ in 90% H_2O/10% D_2O at 10 °C. Samples are the same as Figure 1. Assignments of the imino resonances are indicated. Spectra were acquired with a sweep width of 10000 Hz in 4K complex points. Spectra were obtained with the $1\bar{1}$ spin echo pulse sequence (Sklenář & Bax, 1987) with the delay τ adjusted to give maximum excitation at ~12 ppm, τ = 60 μs, Δ = 50 μs. The FIDs were line broadened by 3 Hz prior to Fourier transformation.

Four imino resonances are observed for each, two G·C and two A·T, from the four sets of two equivalent base pairs. For each complex, large upfield shifts of the imino resonances, indicative of intercalative binding, are observed in the complex relative to the free DNA (Feigon et al., 1984a). Some unshifted imino resonances, corresponding to free DNA, are observed in the spectrum of the saturated complex of CysMeTANDEM with $[d(GGTTAACC)]_2$. This indicates that CysMeTANDEM does not bind as strongly to TTAA sites as to ATAT sites (see Discussion).

Assignments of the Nonexchangeable DNA Resonances in the [d(GGATATCC)]$_2$ Complex. Assignments of the nonexchangeable DNA resonances in the CysMeTANDEM–$[d(GGATATCC)]_2$ were made by analysis of NOESY (Figure 3), COSY (see Figure 7), and HOHAHA (not shown) spectra obtained for the sample in D_2O. The CH5–CH6, TH6–TMe, and deoxyribose spin systems were identified in the COSY and HOHAHA spectra by standard methods (Feigon et al., 1983; Hare et al., 1983; Scheek et al., 1983; Chazin et al., 1986). A NOESY spectrum of the CysMeTANDEM–$[d(GGATATCC)]_2$ complex in D_2O is shown in Figure 3a. The complex gives an exceptionally well-resolved spectrum, with the result that almost all of the resonances could be assigned. The boxed region of the NOESY spectrum, containing the aromatic resonances and their cross peaks to the H1′,CH5 region, is shown expanded in Figure 3b. As anticipated, sequential assignments of the base and H1′,H2′,H2″ protons were interrupted by the intercalation of the quinoxaline rings (Gilbert & Feigon, 1991). Sequential connectivities between the base and H1′ resonances of residues 1–3 and 6–8 were observed and are illustrated in Figure 3a. Although the base–H1′ sequential connectivities are interrupted in the region of the DNA containing residues 4 and 5, a base–base NOE is observed between T_4H6 and A_5H8. This NOE is not ob-

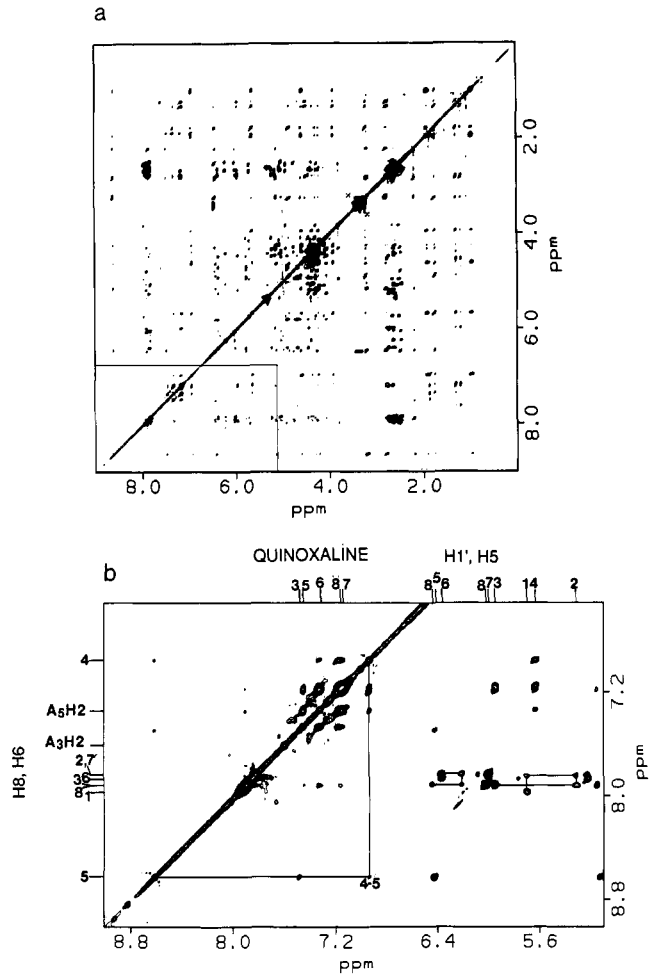

FIGURE 3: (a) NOESY spectrum of the 1:1 CysMeTANDEM-$[d(GGATATCC)]_2$ complex in D_2O at 25 °C with τ_m = 150 ms. (b) Expanded region of the NOESY (boxed region in panel a) showing the aromatic and base–H1′ region. Assignments of the quinoxaline, aromatic, H5, and H1′ resonances are indicated. The base–H1′ sequential connectivities between bases 1 through 3 and between bases 6 through 8, as well as the cross peak between T_4H6 and A_5H8, are indicated by solid lines. Sample conditions were the same as Figure 1. The spectrum was acquired with a sweep width of 5000 Hz in both dimensions, 250 t_1 values of 64 scans, and 2K complex points. A total of 250 points were apodized in both dimensions with a sine-bell phase shifted by 60°. Data in t_1 were zero filled to 1K prior to Fourier transformation.

Table I: Assignments of the [N-MeCys³,N-MeCys⁷]TANDEM–[d(GGATATCC)]$_2$ Complex at 25 °C

	[d(GGATATCC)]$_2$ chemical shifts (ppm)[a]									
	H8/H6	Me/H5/H2	H1′	H2′	H2″	H3′	H4′	H5′,H5″	imino[b]	amino[b]
G_1	7.97		5.71	2.53	2.67	4.94	4.33		12.68	
G_2	7.84		5.33	2.59	2.59	5.08	4.41	4.12, 4.23	12.97	
A_3	7.92	7.60	5.97	2.65	2.76	5.17	4.44	4.26, 4.38		
T_4	6.96	1.88	5.65	0.98	1.93	4.59	3.94	4.38, 4.24	11.49	
A_5	8.62	7.33	6.43	3.21	2.80	5.15	4.60	4.23, 4.37		6.61
T_6	7.86	2.20	6.37	2.63	2.75	5.24	4.46	4.07, 4.30	13.06	
C_7	7.83	6.01	6.22	2.47	2.65	5.04	4.40			7.21, 8.24
C_8	7.91	6.03	6.46	2.51	2.51	4.79	4.27			7.08, 8.47

	CysMeTANDEM chemical shifts (ppm)[a]						
	α	β	β′	γ	γ′	NH[b]	N-Me
serine	5.79	4.68	4.90			8.50	
valine	4.52	2.79		1.21	1.31	8.96	
cysteine	6.47	3.34	3.42				3.23
alanine	4.87	1.52				9.80	
	3	5	6	7	8		
quinoxaline	7.49	7.46	7.33	7.19	7.13		

[a] Chemical shifts relative to DSS. [b] Chemical shifts at 10 °C.

served in the spectra of either of the free DNA octamers (spectra not shown). Using the information from the sequential connectivities and the T_4H6 to A_5H8 cross peak, assignments were obtained for all the H8, H6, and H1′ DNA resonances. Both the A_3H2 and A_5H2 were identified by NOE cross peaks to the A·T imino resonances that are observed in the NOESY in H_2O (Figure 4).

The sequential assignments discussed above were confirmed by connectivities observed between the base and H2′,H2″ resonances (not shown). Sequence-specific assignments for all of the sugar protons except a few H5′,H5″ were obtained by assignment of the previously identified spin systems. The H2′ and H2″ resonances were distinguished from each other on the basis of the intensity of their NOE cross peaks to the H1′, since H1′ proton will always be closer to the H2″ than the H2′ regardless of sugar conformation. The H2′ and H2″ resonances of T_4 and A_5 show unusual chemical shifts. Both the T_4H2′ and T_4H2″ resonances are upfield shifted by ~1 ppm relative to the free DNA. The A_5H2′ proton resonates *downfield* from the A_5H2″ proton, which is the reverse of what is normally seen in DNA and of what is observed for the uncomplexed oligonucleotide (not shown). All of the intranucleotide base–H1′ cross peaks were smaller in intensity than the corresponding base–H2′,H2″ cross peaks, indicating that all of the nucleotides are in the standard anti conformation.

Assignments of the Exchangeable Resonances of the [d-(GGATATCC)]$_2$ Complex. A portion of the NOESY of the CysMeTANDEM–[d(GGATATCC)]$_2$ complex in H_2O which includes the imino and aromatic resonances and all the cross peaks to them is shown in Figure 4. The two A·T iminos resonances were identified by their cross peaks to AH2 resonances and sequence specifically identified from cross peaks observed (via spin diffusion) to their TMe resonance. The most upfield imino has a cross peak to the T_4Me, identifying it as the T_4 imino (Figure 4, box A). This imino is shifted upfield ~2 ppm relative to the T_4 imino on the free DNA (Figure 2a,b), consistent with intercalative binding near the A_5·T_4 base pair. One of the G iminos also has a cross peak to the A_3H2, identifying it as the G_2 imino. The terminal G_1 imino was identified by its large exchange cross peak with water. The C aminos were assigned by cross peaks to the G iminos. The chemical shifts of the nonexchangeable and exchangeable DNA resonances in the CysMeTANDEM–[d(GGATATCC)]$_2$ complex are given in Table I.

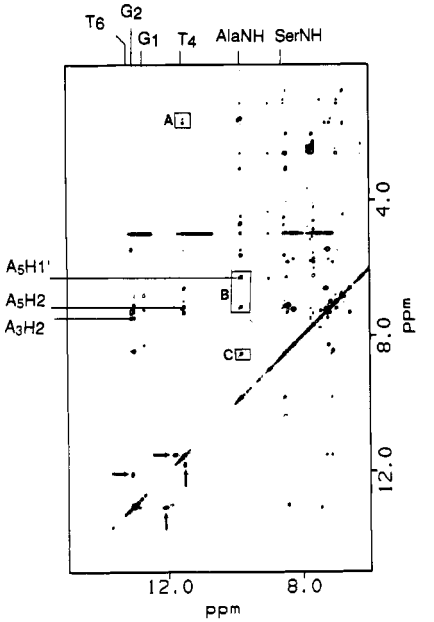

FIGURE 4: Expanded region of the NOESY spectrum in 90% H_2O/10% D_2O of the 1:1 CysMeTANDEM–[d(GGATATCC)]$_2$ complex containing the imino, amino, aromatic resonances and their cross peaks at 10 °C. Sample conditions are the same as Figure 2. Assignments of the iminos, the Ser NH, the Ala NH, the A_5H2, A_5H1′, and the A_3H2 are indicated by solid lines. The boxed cross peak are (a) the T_4 imino to T_4Me and to Ala Me, (b) Ala NH to A_5H2 and to A_5H1′, and (c) Ala NH to Ser NH. Some exchange cross peaks to a small amount of another drug–DNA complex are indicated by arrows. The spectrum was acquired with a sweep width of 10 000 Hz in both dimensions, 300 t_1 values of 64 scans and 4K points. Before processing, the residual water signal was removed from the FIDs by a Gaussian window function with K = 32 and an extrapolation with M = 16 (Marion et al., 1989). A total of 300 points were apodized in both dimensions by sine-bell square phase shifted by 60°.

In addition to expected intracomplex cross peaks, some additional imino–imino cross peaks can be observed in the NOESY spectrum in H_2O (Figure 4). These appear to be exchange cross peaks between the major form of the complex and a very small amount of some other complex (the resonances from this other complex are so small that they do not appear on the diagonal). These additional cross peaks are not observed in the NOESY in H_2O of the related complex between CysMeTANDEM and [d(GATATC)]$_2$ (K. J. Addess and J. Feigon, unpublished results). We speculate that these

Table II: Assignments of the [*N*-MeCys[3],*N*-MeCys[7]]TANDEM–TANDEM–[d(GGTTAACC)]$_2$ Complex at 25 °C

	[d(GGTTAACC)]$_2$ chemical shifts (ppm)[a]									
	H8/H6	Me/H5/H2	H1′	H2′	H2″	H3′	H4′	H5′,H5″	imino[b]	amino[b]
G_1	8.00		5.86	2.63	2.73	4.95	4.33	3.86	12.85	
G_2	7.93		5.96	2.70	2.70	5.08	4.50		12.61	
T_3	6.98	1.41	6.03	2.22	2.49	4.53	4.24		13.05	
T_4	7.01	1.92	5.63	0.96	1.93	4.59	3.89	4.23, 4.32	11.65	
A_5	8.63	7.55	6.26	3.15	2.93	5.14	4.56	4.22, 4.30		6.64
A_6	8.60	7.30	6.54	3.15	3.15	5.30	4.63	3.95, 4.34		
C_7	7.53	5.57	6.15	2.53	2.30	5.02	4.39			7.03, 8.09
C_8	7.86	5.96	6.42	2.47	2.47	4.74	4.26			6.78, 8.07

	CysMeTANDEM chemical shifts (ppm)[a]						
	α	β	β′	γ	γ′	NH[b]	NMe
serine	6.55	4.90	5.05			8.42	
valine	4.44	2.78		1.14	1.30	9.00	
cysteine	6.42	3.35	3.35				3.20
alanine	4.84	1.74				9.66	
	3	5	6	7	8		
quinoxaline	7.55	7.71	7.52	7.38	7.41		

[a] Chemical shifts relative to DSS. [b] Chemical shifts at 10 °C.

are cross peaks between the bis-intercalated drug–DNA complex and a complex in which the drug is binding non-specifically to the DNA.

Assignments of the CysMeTANDEM Resonances in the [d(GGATATCC)]$_2$ Complex. Only one set of Val, Ala, *N*-MeCys, D-Ser, and quinoxaline resonances are observed, indicating that the drug retains its symmetry on binding to the DNA. The four peptide spin systems were identified from the COSY and HOHAHA spectra in D_2O (spectra not shown). The Val amide exchanges slowly with solvent and can be observed in spectra in D_2O. Due to the presence of the modified peptides *N*-MeCys and D-Ser, standard sequential connectivities are not observed around the peptide ring. The sequential connectivities observed in the NOESY spectra in H_2O were Val NH to *N*-MeCys $C_\alpha H$ and Ala NH to D-Ser NH (Figure 4, box C). The assignments of the Ala and Val amides were confirmed from the HOHAHA in H_2O (spectra not shown).

The quinoxaline H5–8 resonances were also identified from the COSY spectra in D_2O. QH3 was identified by its cross peak to the A_5H8. It is the only resonance other than the previously assigned T_4H6 that has a cross peak to the A_5H8 in the aromatic region of the NOESY. The complete assignments of the CysMeTANDEM resonances in the CysMeTANDEM–[d(GGATATCC)]$_2$ complex are listed in Table I.

Assignments of the Resonances of CysMeTANDEM–[d(GGTTAACC)]$_2$ Complex. The DNA and CysMeTANDEM resonances in the [d(GGTTAACC)]$_2$ complex were assigned essentially as described above for the [d(GGATATCC)]$_2$ complex. A portion of a NOESY spectrum in D_2O at 25 °C is shown in Figure 5. Again, sequential connectivities are only observed for bases 1–3 and 6–8, and a base–base connectivity is observed between T_4H6 and A_5H8, consistent with intercalation of the drug at the TpA step as seen for the [d(GGATATCC)]$_2$ complex. As in the case of A_5 in the [d(GGATATCC)]$_2$ complex, the H2′ resonance for the A_5 sugar in the [d(GGAATTCC)]$_2$ occurs upfield from the H2″ resonance (see Figure 7b). The peptides and quinoxaline ring protons in this complex were also assigned essentially as described above.

A portion of the NOESY in H_2O is shown in Figure 6. Again, the most upfield shifted imino resonance is the T_4 imino. The unassigned imino resonances at low field are from some uncomplexed DNA in this sample (Figure 6, box D) as

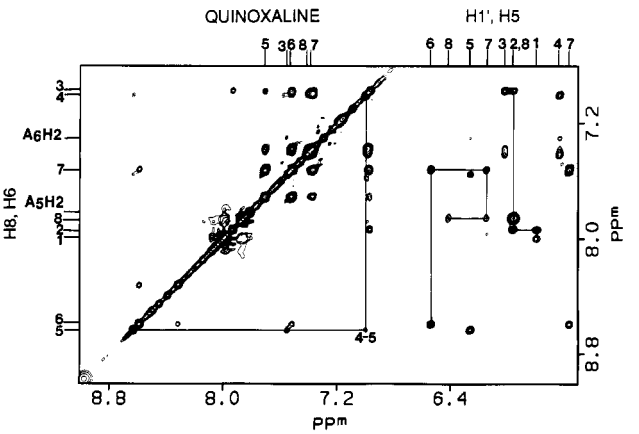

FIGURE 5: Expanded region of the NOESY spectrum (τ_m = 150 ms) of the CysMeTANDEM–[d(GGTTAACC)]$_2$ complex in D_2O at 25 °C, showing the aromatic and the base–H1′ region. The sample is the same as Figure 1. The quinoxaline, aromatic, H5, and H1′ resonances are indicated. The base–H1′ sequential connectivities between bases 1 through 3 and between bases 6 through 8 are indicated by solid lines. The cross peak between A_4H8 and T_5H6 and is labeled. The spectrum was acquired with a sweep width of 5000 Hz in both dimensions, 300 t_1 values of 64 scans, and 2K complex points. A total of 300 points were apodized in both dimensions with a sine-bell phase shifted by 45°. Data in t_1 were zero filled to 1K prior to Fourier transformation.

described above. As was the case for the CysMeTANDEM–[d(GGATATCC)]$_2$ complex, we also see evidence in the imino region of exchange cross peaks between this complex and a small amount of some other complex.

Assignments for the CysMeTANDEM and DNA resonances in the [d(GGTTAACC)]$_2$ complex are given in Table II.

Sugar Conformation in the CysMeTANDEM–[d(GGATATCC)]$_2$ and –[d(GGTTAACC)]$_2$ Complexes. Portions of the P.COSY spectra showing the region containing the H1′–H2′ and H1′–H2″ cross peaks for the CysMeTANDEM complexes with [d(GGATATCC)]$_2$ and [d(GGTTAACC)]$_2$ are shown in Figure 7, panel a and b, respectively. For the CysMeTANDEM–[d(GGATATCC)]$_2$ complex, all of the bases except T_4 have similar cross-peak patterns which show a fine structure typical of a predominantly S-type sugar pucker. (For A_5, the H2″ resonance is upfield of the H2′.) Table III lists the $J_{1'2'}$ and $J_{1'2''}$ coupling constants that were obtained by computer simulations of the P.COSY using the programs

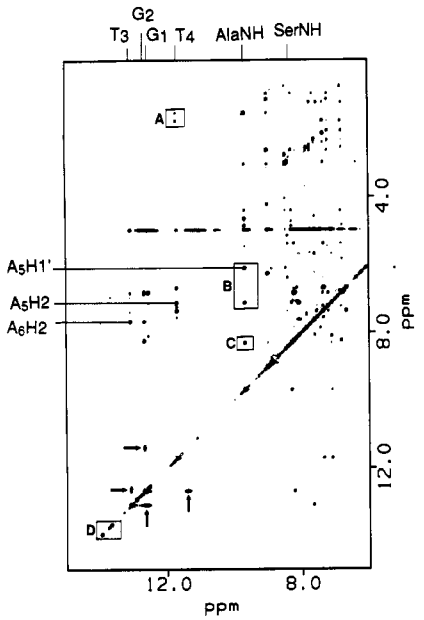

FIGURE 6: Expanded region of the NOESY of the CysMeTANDEM–[d(GGTTAACC)]$_2$ that shows the imino, amino, aromatic resonances and their cross peaks. Assignments of the iminos, the Ser NH, the Ala NH, the A_5H2, A_5H1', and A_6H2 are indicated. The boxed cross peaks are (a) the T_4 imino to T_4Me and to Ala Me, (b) Ala NH to A_5H2 and to A_5H1', and (c) Ala NH to Ser NH. Box D contains the two diagonal peaks for the T iminos of free DNA. Some exchange cross peaks to a small amount of another drug–DNA complex are indicated by arrows. The spectrum was acquired with a sweep width of 10 000 Hz in both dimensions, 300 t_1 values of 64 scans and 4K points. Before processing, the residual water signal was removed from the FIDs by a Gaussian window function with K = 32 and an extrapolation with M = 16 (Marion et al., 1989). A total of 260 points were apodized in both dimensions by sine-bell squared phase shifted by 60°.

Table III

	$J_{1'2'}$	$J_{1'2''}$	$\Sigma 1'$	%S (pS × 100%)
^{1}H–^{1}H Coupling Constants (in Hz) of the Deoxyribose Sugar Rings in CysMeTANDEM–[d(GGATATCC)]$_2$ Complex				
G_1	8.6	6.6	15.2	92
A_2				
T_3	9.2	4.6	13.8	68
A_4	3.5	7.7	11.2	24
T_5	8.9	5.6	14.5	80
A_6	8.9	5.3	14.2	75
C_7	7.7	6.5	14.2	75
C_8				
^{1}H–^{1}H Coupling Constants (in Hz) of the Deoxyribose Sugar Rings in CysMeTANDEM–[d(GGTTAACC)]$_2$ Complex				
G_1	7.6	6.6	14.2	75
G_2				
T_3	7.9	7.1	15.0	88
T_4	3.5	7.7	11.2	24
A_5	8.7	5.4	14.1	73
A_6				
C_7	8.6	6.7	15.2	93
C_8				

SPHINX and LINSHA (Widmer & Wüthrich, 1987). On the basis of the values of $\sum 1'$ and pS listed in Table III, we conclude that T_4 adopts a predominantly N-type (near C3′ endo) sugar pucker, while G_1, A_3, T_5, A_6, and C_7 adopt a predominantly S-type (near C2′ endo) sugar pucker. It was difficult to characterize the geometry of the G_2 and the C_8 sugars from the P.COSY because of the overlap between the 2′ and 2″ resonances. However, in a short mixing time NOESY (τ_m = 50 ms) the base–H3′ cross peaks for G_2 and C_8 are much less intense than the T_4H6–H3′ cross peak. In A-DNA, with a C3′ endo sugar pucker, the TH6–TH3′ distance is shorter than in B-DNA (Wüthrich, 1986). This is consistent with a predominantly S-type conformation for the G_2 and C_8 sugars as well.

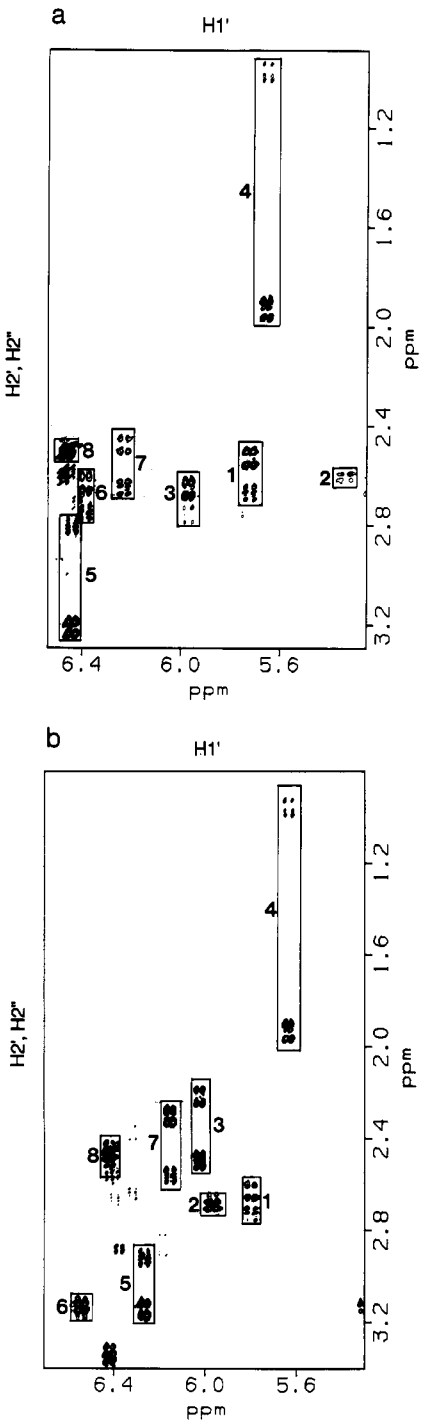

FIGURE 7: Expanded regions of the P.COSY spectra of (a) the CysMeTANDEM–[d(GGTTAACC)]$_2$ complex and (b) the CysMeTANDEM–[d(GGTTAACC)]$_2$ complex showing the region containing the H1′–H2′ and H1′–H2″ cross peaks at 25 °C. Cross peaks for each sugar are boxed and labeled. The spectra were acquired with a sweep width of 5000 Hz in both dimensions, 16 scans per t_1 value, 4K complex points, and 744 and 865 t_1 values, respectively. For each spectrum, a reference spectrum of one t_1 values was acquired with a sweep width of 5000 Hz, 256 scans, and 8K complex points. The reference spectrum was subtracted from each two-dimensional data set. A total of 744 and 865 points, respectively, were apodized with a sine-bell phase shifted by 45°. The data were zero filled to 2K points in t_1 prior to Fourier transformation.

Similar results are observed for the CysMeTANDEM–[d(GGTTAACC)]$_2$ complex. Again, all of the sugars show H1′–H2′ and H1′–H2″ coupling constants indicative of a

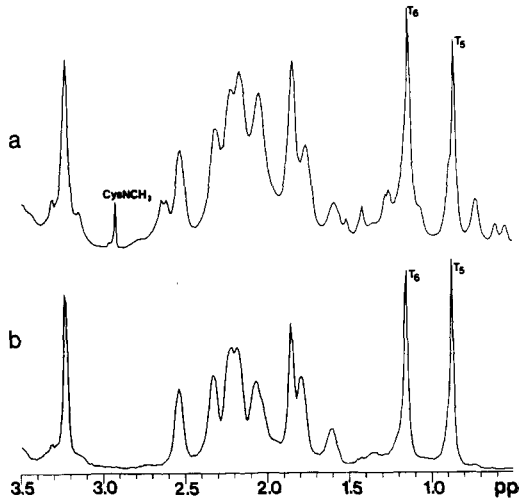

FIGURE 8: ^{1}H NMR spectra of the methylene region of [d-(GGAATTCC)]$_2$ containing (a) no drug and (b) 1 equivalent of CysMeTANDEM at 25 °C. One equivalent of drug in MeOH was added to the free DNA (2 mM duplex, 150 mM NaCl, pH 6.6) in the NMR tube. However, most of the drug precipitated to the bottom of the NMR tube. The spectra were acquired with a sweep width of 5000 Hz in 2K complex points and were line broadened by 3 Hz prior to Fourier transformation.

predominantly S-type sugar pucker with the exception of the T_4 nucleotide 5′ to the TpA binding site. The $J_{1'2'}$, $J_{1'2''}$, $\sum 1'$, and pS values for this complex are listed in Table III. The G_2, A_6, and C_8 H2′ and H2″ resonances overlap, making it difficult to identify their geometries. Again, intensities of the NOESY base–H3′ cross peaks for G2, A6, and C8 are consistent with these sugars having a predominantly S-type sugar pucker.

CysMeTANDEM–DNA Complex Formation with the Sequence [*d(GGAATTCC)*]$_2$. In order to investigate how CysMeTANDEM interacts with a DNA oligonucleotide which contains an ApT but not a TpA site, we added one equivalent of CysMeTANDEM in methanol to a solution of the octamer [d(GGAATTCC)]$_2$. Most of the drug precipitated out of solution during the drying of this sample. A one-dimensional spectrum of the methyl and methylene region of the supernatant is shown in Figure 8a. In comparison with the free DNA shown in Figure 8b, no significant change in the chemical shifts of the DNA occurs upon addition of drug. This result is in contrast to the large changes in the chemical shifts of the DNA resonances observed for the complexes containing a TpA site (Figure 1). However, the spectrum of [d-(GGAATTCC)]$_2$ in the presence of added CysMeTANDEM has significantly broader lines than the spectrum of free DNA. In addition, resonances from the CysMeTANDEM are also present. The *N*-methyl resonance of the *N*-MeCys is labeled on Figure 8a. The intensity of this resonance is much weaker than the intensity of the two DNA TMe resonances. Since CysMeTANDEM is essentially insoluble (6 μM) in aqueous solution, the appearance of the drug resonances in the spectrum of the DNA sample with added CysMeTANDEM and the line broadening observed indicate that CysMeTANDEM is complexed to [d(GGAATTCC)]$_2$. The low solubility indicates that this binding is weak. This result is consistent with the results observed by Powers et al. (1989) for the complex between CysMeTANDEM and the decamer [d-(CCCGATCGGG)]$_2$. However, Powers et al. (1989) did report that the drug binds to their decamer at a ratio of 0.8:1 drug to DNA. The integrated intensity of the *N*-methyl resonance of the *N*-MeCys of the drug compared to the thymine methyl resonances of the DNA indicates that the ratio of drug to DNA in our sample is approximately 0.08:1, which is roughly an order of magnitude less than the ratio of the complex reported by Powers et al. (1989). It is possible that this difference may be due to the difference in the sequence of the two oligonucleotides.

Discussion

Sequence-Specific Binding of CysMeTANDEM to DNA. The NMR data presented here indicate that CysMeTANDEM binds to the TpA step of the octamers [d(GGATATCC)]$_2$ and [d(GGTTAACC)]$_2$ as a bis-intercalator (discussed in detail below). A single symmetric complex is formed for each DNA oligonucleotide. Since the drug binds as a bis-intercalator with the two quinoxaline rings flanking the TpA step, the binding sites in these oligonucleotides can be defined as the four base sites ATAT and TTAA. Although specific binding is observed for both sequences, a fully saturated complex is formed for the ATAT complex only (Figures 1 and 6). Since CysMeTANDEM is essentially insoluble in aqueous solution, it can only be solubilized by specific or nonspecific binding to the DNA. Thus, the smaller amount of the bis-intercalated complex observed with [d-(GGTTAACC)]$_2$ indicates that CysMeTANDEM binds more strongly to ATAT than to TTAA. This difference in binding is probably due to differences in the stacking interactions in the two complexes. Similar results were reported for echinomycin–DNA complexes (Gilbert & Feigon, 1991), where echinomycin was observed to bind more strongly to ACGT than to TCGA sequences.

In addition to the sequence-specific binding of CysMeTANDEM to DNA oligonucleotides containing a TpA site, nonintercalative binding to DNA oligonucleotides is also seen. CysMeTANDEM interacts only weakly, as evidenced by the small amount of drug solubilized, with the DNA oligonucleotide [d(GGAATTCC)]$_2$. Since no intercalative binding was observed for CysMeTANDEM with this oligonucleotide, it can be concluded that ApT is not a bis-intercalation binding site for the antibiotic. Evidence for weak nonintercalative binding of CysMeTANDEM to the oligonucleotides [d-(GGATATCC)]$_2$ and [d(GGTTAACC)]$_2$ was also observed (Figures 4 and 6). Thus, it appears that CysMeTANDEM binds weakly in a nonintercalative and probably nonspecific mode to DNA sequences that are not strong binding sites for intercalative binding.

Bis-Intercalation. The spectral changes and NOE cross peaks observed in these studies indicate that CysMeTANDEM binds specifically to [d(GGATATCC)$_2$] and [d-(GGTTAACC)$_2$] by bis-intercalation of the quinoxaline rings on either side of the central TpA base pairs. In each complex, the T_4 imino is shifted upfield by approximately ~2 ppm and the other T imino by ~0.6–0.9 ppm relative to their chemical shifts in the free DNA, indicative of intercalative binding by the drug (Feigon et al., 1984a). The base–H1′ sequential connectivities are interrupted between bases 3 and 4 and bases 5 and 6 in each complex due to intercalation of the quinoxaline rings at these sites.

Specific binding also results in large upfield shifts of the T_4H2′ and T_4H2″ resonances. Similar upfield shifts were observed for the CH2′ and CH2″ resonances in the CpG binding site of echinomycin–DNA complexes (Gilbert & Feigon, 1991, Gao & Patel, 1988).

In the aromatic region of the NOESY spectrum of the CysMeTANDEM–[d(GGATATCC)]$_2$ complex (Figure 3), NOE cross peaks are observed between QH7, QH6, QH5 and A_3H6, T_4H8. NOE cross peaks are also observed between QH8, QH7, and A_3H2 and between QH7, QH6, QH5, and

T_4Me. These cross peaks indicate that the quinoxaline rings are stacked between the A_3 and T_4 bases. QH3 has a cross peak to the A_5H8, which reveals that the orientation of the long axis of the quinoxaline ring is parallel to the long axis of the A·T base pair. A schematic representation of the stacking of the quinoxaline rings is illustrated in Chart II.

Similarly, in the NOESY spectra of the $[d(GGTTAACC)]_2$ complex, QH7 and QH8 have cross peaks to the T_4H6, while QH6 and QH5 have cross peaks to T_3H6. QH7, QH6, and QH5 have cross peaks to T_3Me and T_4Me. This indicates that the quinoxaline rings are stacked between the T_3 and T_4 bases. QH3 has a cross peak to the A_5H8 in this complex also. Thus, the orientation and stacking of the quinoxaline rings are similar in both the CysMeTANDEM–$[d(GGTTAACC)]_2$ complex and the CysMeTANDEM–$[d(GGATATCC)]_2$ complex as indicated in Chart II. A complete list of the drug–DNA NOEs for each complex is given in Tables IV and V.

Minor Groove Binding. For each complex, the peptide ring binds in the minor groove around the TpA step as evidenced by NOEs between the peptide ring and the minor groove marker protons on the DNA. There are strong NOEs between one of the Val methyls on the peptide ring and the H1′ and H4′ protons from the T_4 and TpA site. There are also strong NOEs between the Ala methyl side chain on the peptide ring and the H1′ and H4′ protons of T_4 and A_5. Similar contacts between the Ala and Val methyl side chains of echinomycin and the minor groove markers of a CpG binding site were observed by Gao and Patel (1988) and by Gilbert and Feigon (1991) in their echinomycin–DNA complexes.

For each complex, the Ala NH resonance is shifted downfield in the H_2O NOESY by approximately 1 ppm, characteristic of hydrogen bonding. Ala NH has strong cross peaks to the AH1′ and AH2 resonances in the TpA step of both complexes (Figures 4 and 6, box B). This lends support to the notion that Ala NH hydrogen bonds to the N3 of adenine. This type of hydrogen bonding has been shown to occur also in CpG-specific drug–DNA complexes such as Triostin A and echinomycin, in which the Ala NH hydrogen bonds to the N3 of guanine (Wang et al., 1984, 1986; Gao & Patel, 1988; Gilbert & Feigon, 1991). The role of this hydrogen bond in the recognition between both CysMeTANDEM and TANDEM and the proposed TpA binding site dinucleotide was probed by Waring and co-workers (Olsen et al., 1986). When they substituted lactic acid for Ala in TANDEM, they found that the drug could no longer protect Tyr 1 from DNase I. This suggests strongly that the binding of TANDEM and CysMeTANDEM to DNA in a sequence-specific manner requires this hydrogen bond.

DNA Conformation in the Complex. The DNA in the CysMeTANDEM–DNA complexes remains essentially in the B-DNA conformation. All of the bases are anti and Watson–Crick base pairs are present in all base pairs of the bis-intercalation complexes. Structural changes observed in the DNA conformation are unwinding of the helix between the central A·T base pairs, buckling of these base pairs, and a change in the sugar pucker of the thymine at the TpA step, as discussed below.

An NOE cross peak is also observed between the T_4H6 and A_4H8 resonances that is not observed in the NOESY spectra of the free DNA octamers under identical conditions. The interproton distance between the T_4H6 and the A_5H8 in both complexes was calculated to be ~4.5 Å by comparing the integrated intensity of the T_4H6–A_5H8 cross peak with the integrated intensities of both of the CH5–CH6 cross peaks. On the basis of a preliminary structure determination of the

Table IV: NOE Cross Peaks Observed between [N-MeCys³,N-MeCys⁷]TANDEM and $[d(GGATATCC)]_2$ in the Complex[a]

	H8/H6	Me/H5/H2	1′	2′	2″	3′	4′	5′5″	amino	imino
G_1										
G_2										
A_3	Q5,Q7 (w); Q6 (m)	Q8 (m); Q7 (w); Ser βH (w); Val Me (m)	Q7 (m); Val Me (s, m)	Q7 (m)	Q7 (s)					
T_4	Q7 (s); Q6 (s); Ala Me (m)	Q7 (m); Q6 (s); Q5 (m)	Q7 (s); Q8 (w); Cys N-Me (w); Ala Me (s); Val Me (s, m)	Val Me (m); Ala Me (m)	Ala Me (m)	Q7 (w)	Q7 (m); Val Me (s, m)			Q5 (s); Q7 (w); Q6 (s);
A_5	Q3 (s)	Ala NH (s); Ser NH (m)	Q3 (m); Ser βH (s); Ala Me (m); Ser αH (s); Ala NH (s);		Ala NH (m)		Ser αH (w)		Q6 (s)	
T_6			Ser βH (s); Ser β′H (s)				Ser αH (m); Ser βH (m); Ser β′H (m)	Ser αH (m); Q7 (m)		Q5 (w)
C_7										
C_8										

[a] Cross-peak intensities are listed as strong (s), medium (m), and weak (w).

Table V: NOE Cross Peaks Observed between [*N*-MeCys^3,*N*-MeCys^7]TANDEM and [d(GGTTAACC)]$_2$ in the Complex[a]

	H8/H6	Me/H5/H2	1′	2′	2″	3′	4′	5′5″	amino	imino
G_1										
G_2										
T_3	Q5 (s); Q6 (m)	Q_5(s); Q6 (s); Q7 (w)	Q7 (w); Q8 (w); Val Me (m, w)	Q7 (s); Q8 (s); Val Me (w, w)	Q7 (s); Q8 (s); Val Me (m, m)					Q5 (s); Q6 (m)
T_4	Q6 (m); Q7 (s); Q8 (m); Ala Me (m)	Q5 (m); Q6 (s)	Q8 (m); Cys *N*-Me (m); Ala αH (w); Ala Me (s)	Ala Me (m); Val Me (m, m)	Ala Me (m); Val Me (m)	Ala Me (s); Val Me (w, w); Ala NH (w)	Q8 (w); Val Me (s, m)	Q8 (s); Val Me (w); Ala Me (w)	Q5 (m); Q6 (s); Q8 (w); Ala Me (m); Ala NH (w); Ser NH (w)	
A_5	Q3 (w)	Ala Me (s); Val Me (m); Ala NH (s)	Ala αH (w); Ala Me (s); Ala NH (s)		Ala NH (m)		Cys *N*-Me (m); Ala Me (m)		Q6 (s)	
A_6										
C_7										
C_8										

[a] Cross-peak intensities are listed as strong (s), medium (m), and weak (w).

related CysMeTANDEM–[d(GATATC)]$_2$ complex [which was calculated using the distance geometry program DSPACE (Hare Research) and refined by energy minimization, restrained molecular dynamics, and calculation of the total relaxation matrix XPLOR (Nilges et al., 1991; K. J. Addess, J. S. Sinsheimer, and J. Feigon, unpublished results)], the TpA step has a helical twist angle of ~−10°. The helical twist angle of standard B-DNA is −36°. Therefore, bis-intercalation of CysMeTANDEM causes an unwinding of the DNA at the TpA step of ~26°. This amount of unwinding would lead to TH6–AH8 interproton distance of ~3.6 Å if the bases remained flat. However, our preliminary structure of the CysMeTANDEM–[d(GATATC)]$_2$ also shows a buckling in these base pairs that moves these protons apart by ~1 Å (unpublished results).

Analysis of the sugar conformations of both CysMeTANDEM complexes reveals that the thymine sugar in the TpA step of the DNA octamers adopt mainly an N-type (near C3′ endo) sugar pucker. These observations are consistent with what Gao and Patel (1988) observed for the C_2 sugar in both echinomycin complexes with [d(ACGT)]$_2$ and with [d(TCGA)]$_2$. Studies of echinomycin complexes with [d(ACGTACGT)]$_2$ and [d(TCGATCGA)]$_2$ by Gilbert and Feigon (1991) also show that cytosine sugars at the CpG binding sites adopt an N-type sugar pucker. Because the thymine sugar of the TpA binding site adopts an N-type geometry, the minor groove width of the DNA at the TpA binding site should be wider than the minor groove width of the free DNA. Widening of the groove should facilitate binding of the peptide in the minor groove at the TpA site and should help stabilize van der Waals interactions between the sugars of the duplex and the amino acids of the octadepsipeptide ring.

Comparison to Previous NMR Results. Powers et al. (1989) studied the binding of CysMeTANDEM with the sequence [d(CGCGATCGCG)]$_2$. On the basis of their work, the authors concluded that CysMeTANDEM binds to the DNA [d(CGCGATCGCG)]$_2$ in a nonintercalative mode in which the drug interacts with the minor groove in the same manner as netropsin or distamycin. However, they detected no NOEs between the drug and the minor groove markers on the DNA. This is not surprising since the DNA studied by Powers et al. (1989) contains the GATC sequence, which was suggested by Waring and co-workers (Low et al., 1986) to not interact with CysMeTANDEM. Because CysMeTANDEM was found to interact with the GTAC restriction site, Waring and co-workers suggested that CysMeTANDEM should bind specifically to TpA steps and not to ApT steps. However, this sequence specificity was not firmly established because echinomycin, which binds specifically to CpG steps, was unexpectedly shown to inhibit the enzyme restricting the GTAC and GATC restriction sites. For this reason, we studied the interaction between CysMeTANDEM and the octamer [d(GGAATTCC)]$_2$, which contains an ApT site but not a TpA site. The spectra shown in Figure 8 indicate that CysMeTANDEM binds weakly to DNA which does not contain a TpA step, consistent with the results reported by Powers et al. (1989). Because of the small amount of complex formed, we could not study the interaction between CysMeTANDEM and the octamer [d(GGAATTCC)]$_2$ in detail, and we cannot make any firm conclusions about the specificity or conformation of the nonintercalative mode of drug binding.

Comparison with the Crystal Structure of TANDEM and the Model Studies of TANDEM–DNA Complexes. On the basis of the crystal structure of TANDEM, Viswamitra et al.

(1981) noted two important structural features of the drug that could play an important role in its sequence specificity. The first feature is that TANDEM contains an intramolecular hydrogen bond between the Val NH and the Ala carbonyl. According to Singh et al. (1986), the presence of this hydrogen bond places the carbonyl in an unfavorable position to accept a hydrogen bond from the guanine exocyclic C2 amino group. The second structural feature is that the NH bond of Ala would be positioned parallel to the plane of the quinoxaline rings when they are sandwiched between DNA bases. Viswamitra et al. (1981) used these structural features to build models of several TANDEM–DNA complexes. They concluded from these studies that TANDEM should bis-intercalate at an ApT step, resulting in an intermolecular hydrogen bond between the Ala NH and thymine O2.

Our results suggest that these two structural features are important in the sequence-specific binding of CysMeTANDEM to a TpA step and not to an ApT step. The Val amide resonance is so slowly exchanging that it can be seen after the sample has been in D_2O for several days, and it has no intermolecular NOEs with any minor groove marker protons of the DNA. This indicates that the Val amide must form an intramolecular hydrogen bond with the Ala carbonyl. This suggests that CysMeTANDEM and TANDEM have the same structures both in solution and in the crystal and that the orientation of the Ala NH of both drugs with respect to their quinoxaline rings is the same. Furthermore, the Cys *N*-methyl has little interaction with the DNA in both complexes, having only one NOE to the TH1′ proton of the TpA step in both complexes. This indicates that *N*-MeCys probably plays an insignificant role in the drug's binding specificity. In our preliminary structure of the CysMeTANDEM–[d(GATATC)]$_2$ complex, the Cys *N*-methyl faces 90° relative to the face of the Ala methyl, positioning it out of the minor groove. This would explain why the Cys *N*-methyl has strong NOEs to the Ala methyl, while having little interaction with the DNA. For these reasons, we predict that TANDEM also should bind specifically to a TpA step as a bis-intercalator with the Ala NH of TANDEM hydrogen bonding to the N3 of adenine, in contrast to the model put forth by Viswamitra et al. (1981).

Summary

The NMR studies reported here show unambiguously that sequence-specific bis-intercalative binding of CysMeTANDEM occurs on either side of a TpA step. Only nonspecific binding is observed for DNA without a TpA step, including those DNA oligonucleotides containing ApT sequences. A complete three-dimensional structure based on NMR distance constraints is currently being determined for the complex of CysMeTANDEM with [d(GATATC)]$_2$. This structure should provide further insight into factors determining the sequence-specific binding of CysMeTANDEM with DNA.

Registry No. [*N*-MeCys³,*N*-MeCys⁷]TANDEM, 137918-30-0; d(GGATATCC), 99221-83-7; d(GGTTAACC), 68892-56-8; d(GGAATTCC), 70755-49-6.

References

Aue, W., Bartholdi, E., & Ernst, R. R. (1976) *J. Chem. Phys. 64*, 2229–2246.

Bax, A., & Davis, D. G (1985) *J. Magn. Reson. 65*, 355–360.

Bax, A., & Lerner, L. (1988) *J. Magn. Reson. 79*, 429–438.

Chakravarty, P. K., & Olsen, R. K. (1978) *Tetrahedron Lett. 19*, 1613–1616.

Chazin, W. J., Wüthrich, K., Hybert, S., Rance, M., Denny, W. A., & Leupin, W. (1986) *J. Mol. Biol. 190*, 439–453.

Feigon, J., Leupin, W., Denny, W. A., & Kearns, D. R. (1983) *Biochemistry 22*, 5943–5951.

Feigon, J., Leupin, W., Denny, W. A., & Kearns, D. R. (1984a) *J. Med. Chem. 27*, 450–465.

Fox, K. R., Olsen, R. K., & Waring, M. J. (1982) *Biochim. Biophys. Acta 696*, 315–322.

Gao, X., & Patel, D. J. (1988) *Biochemistry 27*, 1744–1751.

Gilbert, D. E., & Feigon, J. (1991) *Biochemistry 30*, 2483–2494.

Gilbert, D. E., van der Marel, G. A., van Boom, J. H., & Feigon, J. (1989) *Proc. Natl. Acad. Sci. U.S.A. 86*, 3006–3010.

Hare, D. R., Wemmer, D. E., Chou, S. H., Drobny, G., & Reid, B. R. (1983) *J. Mol. Biol. 171*, 319–336.

Katagiri, K., Yoshida, T., & Sato, K. (1975) in *Antibiotics III. Mechanism of Action of Antimicrobial and Antitumor Agents* (Corcoran, J., & Hahn, F. E., Eds.) pp 234–251, Springer-Verlag, Berlin, Heidelberg, and New York.

Kintanar, A., Klevit, R. E., & Reid, B. R. (1987) *Nucleic Acids Res. 15*, 5845–5861.

Kumar, A., Ernst, R. R., & Wüthrich, K. (1980) *Biochem. Biophys. Res. Commun. 95*, 1–6.

Lee, J. S., & Waring, M. J. (1978a) *Biochem. J. 173*, 115–128.

Lee, J. S., & Waring, M. J. (1978b) *Biochem. J. 173*, 129–144.

Low, C. M. L., Olsen, R. K., & Waring, M. J. (1984a) *FEBS Lett. 176*, 414–419.

Low, C. M. L., Drew, H. R., & Waring, M. J. (1984b) *Nucleic Acids Res. 12*, 4865–4879.

Low, C. M. L., Fox, K. R., Olsen, R. K., & Waring, M. J. (1986) *Nucleic Acids Res. 14*, 2015–2033.

Marion, D., & Bax, A. (1988) *J. Magn. Reson. 80*, 528–533.

Marion, D., Ikura, M., & Bax, A. (1989) *J. Magn. Reson. 84*, 425–430.

Mueller, L. (1987) *J. Magn. Reson. 72*, 191–196.

Nilges, M., Habazettl, J., Brünger, A. T., & Holak, T. A. (1991) *J. Mol. Biol. 219*, 499–510.

Olsen, R. K., Ramasamy, K., Bhat, K. L., Low, C. M. L., & Waring, M. J. (1986) *J. Am. Chem. Soc. 108*, 6032–6036.

Otting, G., Widmer, H., Wagner, G., & Wüthrich, K. (1986) *J. Magn. Reson. 66*, 187–193.

Powers, R., Olsen, R. K., & Gorenstein, D. G. (1989) *J. Biomol. Struct. Dyn. 7*, 515–553.

Rinkel, L. J., & Altona, C. (1987) *J. Biomol. Struct. Dyn. 4*, 621–649.

Scheek, R. M., Russo, N., Boelens, R., & Kaptein, R. (1983) *J. Am. Chem. Soc. 105*, 2914–2915.

Singh, U. C., Pattabiraman, N., Langridge, R., & Kollman, P. A. (1986) *Proc. Natl. Acad. Sci. U.S.A. 83*, 6402–6406.

Sklenář, V., & Bax, A. (1987) *J. Magn. Reson. 75*, 378–383.

States, D. J., Haberkorn, R. A., & Ruben, D. J. (1982) *J. Magn. Reson. 48*, 286–292.

Ughetto, G., Wang, A. H.-J., Quigley, G. J., van der Marel, G. A., van Boom, J. H., & Rich, A. (1985) *Nucleic Acids Res. 13*, 2305–2323.

van Dyke, M. M., & Dervan, P. B. (1984) *Science 225*, 1122–1127.

Viswamitra, M. A., Kennard, O., Cruse, W. B. T., Egert, E., Sheldrick, G. M., Jones, P. G., Waring, M. J., Wakelin, L. P. G., & Olsen, R. K. (1981) *Nature 289*, 817–819.

Waring, M. J. (1979) in *Antibiotics* (Hahn, F. E., Ed.) Vol. 5, Part 2, pp 173-194, Springer-Verlag, Berlin, Heidelberg, and New York.
Wang, A. H.-J., Ughetto, G., Quigley, G. J., Hakoshima, T., van der Marel, G. A., van Boom, J. H., & Rich, A. (1984) *Science 225*, 1115-1121.
Wang, A. H.-J., Ughetto, G., Quigley, G. J., & Rich, A. (1986) *J. Biomol. Struct. Dyn. 4*, 319-342.
Widmer, H., & Wüthrich, K. (1987) *J. Magn. Reson. 74*, 316-336.
Wüthrich, K. (1986) *NMR of Proteins and Nucleic Acids*, Wiley, New York.

Metal Activation of Synthetic and Degradative Activities of ϕ29 DNA Polymerase, a Model Enzyme for Protein-Primed DNA Replication†

José A. Esteban, Antonio Bernad, Margarita Salas,* and Luis Blanco
Centro de Biologia Molecular (CSIC-UAM), Universidad Autônoma, Canto Blanco, 28049 Madrid, Spain
Received June 28, 1991; Revised Manuscript Received September 26, 1991

ABSTRACT: Analysis of metal activation on the synthetic and degradative activities of ϕ29 DNA polymerase was carried out in comparison with T4 DNA polymerase and *Escherichia coli* DNA polymerase I (Klenow fragment). In the three DNA polymerases studied, both the polymerization and the 3′→5′ exonuclease activity had clear differences in their metal ion requirements. The results obtained support the existence of independent metal binding sites for the synthetic and degradative activities of ϕ29 DNA polymerase, according with the distant location of catalytic domains (N-terminal for the 3′→ 5′ exonuclease and C-terminal for DNA polymerization) proposed for both Klenow fragment and ϕ29 DNA polymerase. Furthermore, DNA competition experiments using ϕ29 DNA polymerase suggested that the main differences observed in the metal usage to activate polymerization may be the consequence of metal-induced changes in the enzyme–DNA interactions, whose strength distinguishes processive and nonprocessive DNA polymerases. Interestingly, the initiation of DNA polymerization using a protein as a primer, a special synthetic activity carried out by ϕ29 DNA polymerase, exhibited a strong preference for Mn^{2+} as metal activator. The molecular basis for this preference is mainly the result of a large increase in the affinity for dATP.

It has long been known that metal ions are required cofactors for the catalytic activities of DNA polymerases, i.e., DNA polymerization and exonuclease activity (Bessman et al., 1958; Lehman & Richardson, 1964). Mg^{2+}-activated catalysis has been the one most extensively studied, since, in general, it yields the highest activity. However, it has been demonstrated that other metal ions like Mn^{2+}, Co^{2+}, Ni^{2+}, or Zn^{2+} can also serve as activators for DNA polymerases in vitro (Sirover & Loeb, 1976; Burgers & Eckstein, 1979), being presently unknown which metal or metals are used in vivo.

Determination of metal ion requirements of DNA polymerases becomes complex by the fact that metals not only bind and activate DNA polymerases but also bind to DNA and dNTPs, leading to different template and substrate complexes depending on the metal ion and on its concentration (Murray & Flessel, 1976; Marzilli et al., 1980; Sigel, 1987).

The location of the polymerization active site of *Escherichia coli* DNA polymerase I Klenow fragment (pol I K) relies on biochemical and genetic studies (Joyce & Steitz, 1987; Polesky et al., 1990), as well as on recent X-ray crystallographic analysis showing dCTP bound to the enzyme; in this case, Gln-708 and Glu-710 are involved in metal ion binding (L. Beese, J. Friedman, and T. A. Steitz, personal communication). Furthermore, using a different approach, a single metal binding site has been detected in the presence of dGTP (Mullen et al., 1990). In the C-terminal domain of ϕ29 DNA polymerase and other α-like DNA polymerases from distantly related organisms, a highly conserved amino acid sequence motif (YGDTDS) has been proposed to be part of the metal binding site for polymerization (Argos, 1988; Bernad et al., 1990). However, the role for this metal in binding dNTPs and primer substrates and/or catalysis is not yet clear.

In the case of the 3′→ 5′ exonuclease activity, a detailed understanding of the structural basis of the metal ion requirements has been provided by crystallographic analysis of pol I K complexed with ssDNA (Freemont et al., 1988). The pol I K exonuclease active center contains two binding sites for metal ions: one metal ion (site A) is coordinated by the carboxylate groups of Asp-355, Glu-357, and Asp-501, the fourth ligand being the phosphate of the bond to be cleaved; a second metal ion (site B) is located between this phosphate and the carboxylate of Asp-424. Further support of the relevance of these residues involved in metal binding is the fact that they are conserved in many prokaryotic and eukaryotic DNA polymerases (Bernad et al., 1989). Thus, the putative residues involved in metal binding for both polymerase and exonuclease activities appear among the best conserved ones

†This investigation has been aided by Research Grant 5R01 GM27242-12 from the National Institutes of Health, by Grant PB87-0323 from Dirección General de Investigación Cientifica y Técnica, and by an institutional grant from Fundación Ramón Areces. J.A.E. was the recipient of a fellowship from Plan de Formación de Personal Investigador, and A.B. was a postdoctoral fellow from Consejo Superior de Investigaciones Cientificas.
* Correspondence should be addressed to this author.

[1] Abbreviations: pol I K, *E. coli* DNA polymerase I Klenow fragment; ssDNA, single-stranded DNA; dsDNA, double-stranded DNA; p3–DNA, ϕ29 DNA–terminal protein complex; DTT, dithiothreitol; BSA, bovine serum albumin; SDS, sodium dodecyl sulfate.

0006-2960/92/0431-350$03.00/0